

Resonance magnetoelectric effects in layered magnetostrictive-piezoelectric composites

M. I. Bichurin, D. A. Filippov, and V. M. Petrov

Department of Physics and Engineering, Novgorod State University, B. S. Peterburgskaya St. 41, 173003 Veliky Novgorod, Russia

V. M. Laletsin and N. Paddubnaya

Institute of Technical Acoustics, National Academy of Sciences of Belarus, 210717 Vitebsk, Belarus

G. Srinivasan

Physics Department, Oakland University, Rochester, Michigan 48309, USA

(Received 14 May 2003; revised manuscript received 2 July 2003; published 15 October 2003)

Magnetolectric interactions in bilayers of magnetostrictive and piezoelectric phases are mediated by mechanical deformation. This work is concerned with the theory and companion data for magnetolectric (ME) coupling at electromechanical resonance (EMR) in the layered samples. Estimated ME voltage coefficient versus frequency profiles for nickel, cobalt, or lithium ferrite and lead zirconate titanate (PZT) predict a giant ME effect at EMR with the highest coupling expected for cobalt ferrite-PZT. There is excellent agreement between the theory and data for layered nickel ferrite-PZT; the ME voltage coefficient at resonance increases by a factor of 40 compared to low frequency values. Similar measurements on layered ferromagnetic alloy-PZT and bulk ferrite-PZT reveal even a stronger EMR assisted enhancement in ME coupling.

DOI: 10.1103/PhysRevB.68.132408

PACS number(s): 75.80.+q, 75.50.Gg, 75.60.-d, 77.65.-j

There has been renewed interest in recent years in the phenomenon of magnetolectric (ME) effect in ferromagnetic-ferroelectric heterostructures. The effect facilitates the conversion between energies stored in magnetic and electric fields and is rather strong in layered systems compared to single phase materials or bulk composites.¹⁻¹⁰ The absence of a substantial leakage current in layered composites, coupled with ease of poling, lead to an enhancement of piezoelectric and ME effects. Systems studied so far include transition and rare-earth metals and alloys, lanthanum manganites, or ferrites for the magnetic phase and barium titanate, lead zirconate titanate (PZT) or polyvinylidene fluoride (PVDF) for the piezoelectric phase.⁵⁻¹⁰ Studies have focused on dynamic ME coupling at low frequencies (10–1000 Hz). For such measurements, the sample is initially poled in an electric field E perpendicular to the plane and is then subjected to a bias field H and an ac field δH . The mechanical deformation due to ac magnetostriction is coupled to the ferroelectric phase, resulting in an electric field δE across the sample thickness. The ME voltage coefficient $\alpha_E = \delta E / \delta H$ is measured for longitudinal (all the fields parallel to each other) or transverse (H and δH perpendicular to E and δE) fields. Data on α_E as a function of H , in general, shows a peak at some H_m when the ac magnetostriction is maximum, and the ME coupling vanishes when the magnetostriction attains saturation.⁵⁻¹⁰

Although studies on ME interactions in bulk composites date back to early 1970s and layered systems to the 1990s, there is lack of information on its frequency dependence. The frequency range of our particular interest is the one that covers the electromechanical resonance (EMR). We performed such measurements over $f = 10$ Hz–500 kHz on multilayers of nickel ferrite (NFO)-PZT and the results are shown in Fig. 1. The data are for a 10-mm-diameter disk that contained 11 layers of 13- μm -thick NFO and 10 layers of PZT with a thickness of 26 μm . It was poled with an electric field E

perpendicular to the sample plane. We first measured the longitudinal voltage coefficient $\alpha_{E,L}$ versus H at 100 Hz that showed a peak voltage coefficient of 30 mV/cm Oe at $H_m = 1050$ Oe. Then for H set at H_m , $\alpha_{E,L}$ was measured as a function of f . The profile in Fig. 1 shows resonance at f_r

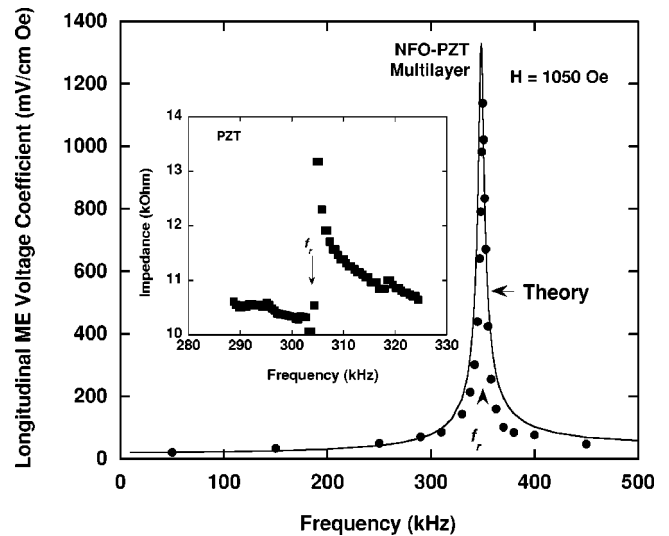


FIG. 1. Variations in longitudinal magnetoelectric (ME) voltage coefficients with frequency f for a multilayer of nickel ferrite-PZT. The sample contained 11 layers of ferrite of thickness 13 μm and 10 layers of PZT with a thickness of 26 μm . The longitudinal coefficient $\alpha_{E,L} = \delta E / \delta H$ corresponds to bias field H , ac field δH , and the induced electric field δE all along the direction 3, perpendicular to sample plane. The bias field H was set for maximum ME coupling. The peak in $\alpha_{E,L}$ arises due to electromechanical resonance (EMR) associated with radial modes in the composite. The solid line is the calculated values based on the present theory. The inset, impedance vs. f data for a 10-mm disk of PZT, shows the manifestation of EMR at a frequency close to the resonance in $\alpha_{E,L}$ for the composite. The arrows indicate the resonance frequency f_r .

$=350$ kHz with a maximum $\alpha_{E,L}$ of 1200 mV/cm, a factor of 40 higher than low frequency values. We identified the peak in $\alpha_{E,L}$ with EMR in PZT in the multilayer. Electromechanical resonance in piezoelectric phases is investigated through measurements of impedance z or dielectric constant as a function of frequency. Figure 1 shows such z versus f data for a 10-mm-diameter disc of PZT. One observes a discontinuity in z due to EMR associated with the radial modes in PZT. The resonance occurs at a frequency close to the peak position in $\alpha_{E,L}$ versus f in Fig. 1. Here we are concerned with the theory for the resonance in $\alpha_{E,L}$.

This work constitutes the first theoretical modeling of the resonance ME coupling in Fig. 1. Significant studies on frequency dependence of ME susceptibility include the works by Tilley and Scott on single crystal BaMnF₄ and our model for ME coupling at ferromagnetic resonance (FMR) in ferrite-PZT bilayers.^{11–13} Using the Landau-Lifshitz equations of motion, the ME susceptibility was estimated for the low temperature phase of BaMnF₄. It was shown that microwave-magnon frequency decreases and the optical-phonon frequency increases with the strength of the ME coupling. The magnetic, dielectric, and magnetoelectric susceptibilities were found to have poles at both magnon and phonon frequencies.^{11,12} We developed a phenomenological theory for ME coupling at FMR in ferroelectric/ferromagnetic layered structures. Expressions relating the magnetic and ME susceptibility to ME coupling constants were obtained. The theory predicts a unique resonance in the electric field dependence of the magnetic susceptibility.¹³ The resonance phenomenon considered here occurs at 100 kHz to 10 MHz, much smaller than magnon, optical-phonon, or FMR frequencies.

A ferromagnetic-ferroelectric bilayer is assumed in which the induced polarization δP is related to the field δH by $\delta P = \alpha \delta H$, where α is the ME susceptibility. The ME voltage coefficient α_E is related to α by the expression $\alpha = \epsilon_0 \epsilon_r \alpha_E$, where ϵ_r is the relative permittivity of the material. The model is for radial modes and longitudinal field configuration. An averaging procedure is employed to obtain the composite parameters and the voltage coefficient $\alpha_{E,L}$. The theory is then applied to bilayers containing ferrites of importance, i.e., cobalt ferrite (CFO) due to high magnetostriction, nickel ferrite (NFO) due to strong magnetomechanical coupling, and lithium ferrite (LFO) because of low loss characteristics. Based on the model, one expects a resonance character in $\alpha_{E,L}$ versus frequency profile with the strongest ME coupling at f_r for CFO-PZT and the weakest coupling for LFO-PZT.

The composite is assumed to be a homogeneous medium that can be described by effective parameters, such as compliance, piezoelectric, and magnetostrictive coefficients that are determined from parameters for individual phases. The assumption is valid when the layer thickness is small compared to wavelengths for the acoustic modes and is certainly true for EMR that occurs at 100–500 kHz. The bilayer geometry is a thin disk in the (1,2) plane with a radius R and thickness t . The electrodes are assumed to be of negligible thickness and the longitudinal fields are along the direction 3. The ac magnetic field induces harmonic waves in the ra-

dial or thickness modes. It is supposed that $t \ll R$ so that only radial modes are considered. For a thin disk, it is possible to neglect any pressure variation along the transverse direction. The axial symmetry results in nonzero components of the pressure and strain tensors T_{rr} , $T_{\theta\theta}$, S_{rr} , and $S_{\theta\theta}$. The generalized Hooke's law and corresponding equations have the following form:

$$\begin{aligned} S_{rr} &= s_{11}T_{rr} + s_{12}T_{\theta\theta} + d_{31}E_z + q_{31}H_z, \\ S_{\theta\theta} &= s_{12}T_{rr} + s_{11}T_{\theta\theta} + d_{31}E_z + q_{31}H_z, \\ D_z &= d_{31}(T_{rr} + T_{\theta\theta}) + \epsilon_{33}E_z + \alpha_{33}H_z, \end{aligned} \quad (1)$$

where $S_{rr} = \partial u_r / \partial r$, $S_{\theta\theta} = (1/r)u_r$, u_i is displacement coordinate of medium, T_{ij} is stress tensor component, s_{ij} is compliance coefficient, q_{ij} and d_{ij} are piezomagnetic and piezoelectric coefficients, D_i is electric displacement component, ϵ_{ij} is permittivity matrix, and α_{33} is the ME coefficient. The equation of elastodynamics has the following form for the radial propagating mode:

$$\frac{dT_{rr}}{dr} + \frac{1}{r}(T_{rr} - T_{\theta\theta}) + \rho\omega^2 u_r = 0, \quad (2)$$

where ρ is the density and ω is the angular frequency. Solutions of the Eq. (2), taking into account Eq. (1), can be presented as superposition of the first and second order Bessel functions. Using the boundary conditions: $u_r = 0$ at $r = 0$ and $T_{rr} = 0$ at $r = R$ we get expressions for T_{rr} and $T_{\theta\theta}$:

$$T_{rr} = \frac{1}{s_{11}(1-\nu)} \left[\frac{kR J_0(kr) - (1-\nu) \frac{R}{r} J_1(kr)}{\Delta_r} - 1 \right] \times (q_{31}H_z + d_{31}E_z) \quad (3)$$

$$T_{\theta\theta} = \frac{1}{s_{11}(1-\nu)} \left[\frac{\nu kR J_0(kr) + (1-\nu) \frac{R}{r} J_1(kr)}{\Delta_r} - 1 \right] \times (q_{31}H_z + d_{31}E_z), \quad (4)$$

where $k = \sqrt{\rho s_{11}(1-\nu^2)}\omega$, $\nu = -s_{12}/s_{11}$ is Poisson's ratio, and $\Delta_r = kR J_0(kR) - (1-\nu)J_1(kR)$.

The electric field, obtained by taking into consideration open circuit conditions, i.e., $\int_S D_n dS = 0$, where S is electrode plane, is

$$E_z = \frac{1}{|\Delta_a|} \left[\frac{2d_{31}q_{31}}{\epsilon_{33}s_{11}(1-\nu)} \left(\frac{(1+\nu)J_1(kR)}{\Delta_r} - 1 \right) + \frac{\alpha_{33}}{\epsilon_{33}} \right] H_z, \quad (5)$$

where

$$\Delta_a = 1 - K_p^2 + K_p^2(1+\nu)J_1(kR)/\Delta_r + i\Gamma, \quad (6)$$

$K_p^2 = 2d_{31}^2/\epsilon_{33}s_{11}(1-\nu)$ is the coefficient of electromechanical coupling for radial mode, and Γ is the loss factor. Finally, the longitudinal ME voltage coefficient $\alpha_{E,L} = \delta E_3 / \delta H_3$, is obtained as

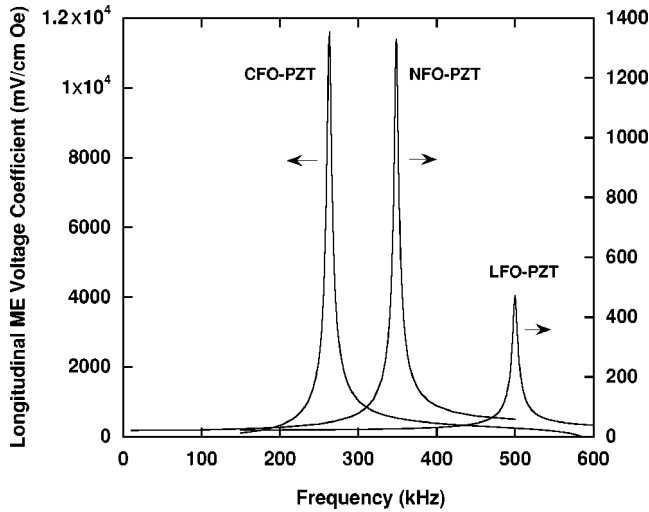


FIG. 2. Theoretical longitudinal ME voltage coefficient $\alpha_{E,L}$ as a function of the frequency of the ac field for bilayers of ferrite and PZT. Estimates are for sample thickness much smaller than the radius. The diameter of the bilayer samples are 12 mm for cobalt ferrite (CFO)-PZT, 10 mm for nickel ferrite (NFO)-PZT, and 8 mm for lithium ferrite (LFO)-PZT. Notice the resonance in $\alpha_{E,L}$ vs. f at the electromechanical resonance frequency. Parameters used for the estimates are given in Table I.

$$\alpha_{E,L} = -\frac{1}{|\Delta_a|} \left[\frac{2d_{31}q_{31}}{\epsilon_{33}s_{11}(1-\nu)} \left(\frac{(1+\nu)J_1(kR)}{\Delta_r} - 1 \right) + \frac{\alpha_{33}}{\epsilon_{33}} \right]. \quad (7)$$

Analysis of Eq. (7) shows that the first term in square brackets is negligible at low frequencies and the dynamic ME coefficient coincides with its low frequency (static) value of $\alpha_{33}/\epsilon_{33}$. At EMR, however, the first term dominates; the resonance frequency is determined by the condition $\text{Re} \Delta_a = 0$ and the ME voltage coefficient is expected to show a peak at this frequency. It follows from Eq. (6) that the resonance frequency depends on sample radius and the following material parameters: compliances s_{11} and s_{12} , density ρ , and coefficient of electromechanical coupling for radial mode K_p . The peak value of $\alpha_{E,L}$ and resonance linewidth are determined by effective piezomagnetic (q_{31}) and piezoelectric (d_{31}) coefficients, compliances, permittivity, and loss factor.

We next apply the theory to representative ferrite-PZT bilayers. The ferrites considered include cobalt ferrite because of high magnetostriction and piezomagnetic coupling, nickel ferrite due to strong magneto-mechanical coupling, and lithium ferrite.^{3,6} Estimated $\alpha_{E,L}$ versus f values are

shown in Fig. 2 for parameters in Table I. Calculations are for a PZT volume fraction of 0.7, effective composite parameters in Ref. 5, and a bias field H that corresponds to maximum piezomagnetic coupling q . The sample diameter has been chosen in such a way as to separate the EMR for the bilayers. A resonance character is clearly evident in Fig. 2; the peak α_E is the highest for CFO-PZT due to high piezomagnetic coupling and is the lowest for LFO-PZT. The most important inference from Fig. 2 is the overall enhancement in α_E at resonance.

Measurements of ME effects at EMR are discussed next. We first consider the data in Fig. 1 for NFO-PZT multilayers with a PZT volume fraction of 0.7. Estimates based on the current theory are shown for comparison. The resonance occurs at 350 kHz, in agreement with calculated values for sample dimension and composite parameters in Table I. The theoretical profile for a loss factor $\Gamma=0.08$ tracks the observed variation in $\alpha_{E,L}$ with f . The most significant inference in Fig. 1 is the realization of predicted giant ME interactions in the composite at EMR. The $\alpha_{E,L}$ at resonance is 1200 mV/cm Oe and must be compared with the low-frequency value of 30 mV/cm Oe. Although the theoretical $\alpha_{E,L}$ at EMR is 15% higher than the measured value, the overall agreement between theory and data is excellent.

Similar studies, however, revealed a even stronger resonance in ME interactions in layered ferromagnetic alloy-PZT composites. Permendur (49% Fe, 49% Co, 2% V), a soft magnetic alloy with a high magnetostriction, was used for the magnetic phase.¹⁴ Measurements of $\alpha_{E,L}$ vs f were done on a 9 mm diameter disk of Permendur-PZT-Permendur trilayer and are shown in Fig. 3. The bias field H was set at $H_m = 600$ Oe. The profile shows resonance at 330 kHz with a maximum $\alpha_{E,L}$ of 8 V/cm, which is a factor of 200 higher than low-frequency values. The resonance frequency compares favorably with the results in Fig. 1 for NFO-PZT, but α_E at resonance is much higher than for NFO-PZT primarily due to superior magnetostriction and magneto-mechanical coupling parameters for Permendur.

Another significant finding of relevance to the present study concerns the resonance ME effect in bulk ferrite-PZT composites. Although one expects a similar EMR associated enhancement in $\alpha_{E,L}$ for bulk samples, a theoretical model for the phenomenon in bulk composites is yet to be developed. Such a task is complicated by the fact that boundary conditions at the interface between the two phases are dependent on the volume fraction, particle shape and specific mechanical connectivity. Here we provide data for resonance in $\alpha_{E,L}$ vs f for bulk samples consisting of modified nickel fer-

TABLE I. Compliance coefficient s , piezomagnetic coupling q , piezoelectric coefficient d , and permittivity ϵ for cobalt ferrite (CFO), nickel ferrite (NFO), lithium ferrite (LFO), and lead zirconate titanate (PZT).

Material	s_{11} (10^{-12} m ² /N)	s_{12} (10^{-12} m ² /N)	q_{31} (10^{-12} m/A)	d_{31} (10^{-12} m/V)	ϵ_{33}/ϵ_0
CFO	6.5	-2.4	556		10
NFO	6.5	-2.4	125		10
LEO	3.3	-1.65	-12.5		10
PZT	15.3	-5		-175	1750

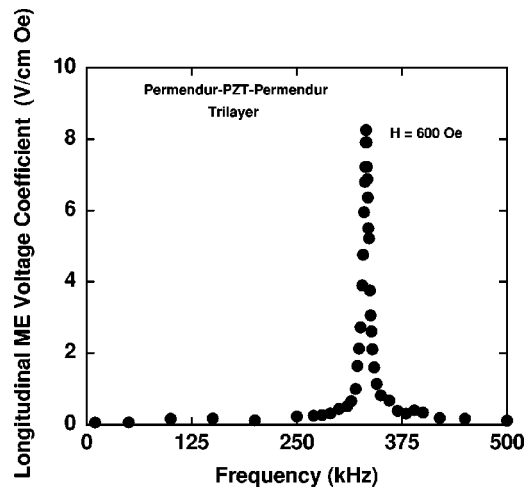


FIG. 3. Variations in longitudinal magnetoelectric (ME) voltage coefficients with the frequency for a trilayer of Permendur-PZT-Permendur. The thickness of Permendur and PZT are 0.18 mm and 0.36 mm, respectively. The lines are guide to the eye.

rite and PZT. It was necessary to modify NFO with a combination of substitutions and Fe deficiency to increase the electrical resistivity. The high resistivity leads to excellent poling characteristics and strengthens ME interactions.³ Samples with PZT concentration varying from 10 to 90 wt. % were studied. Magnetoelectric voltage coefficients were measured at low frequencies (1 kHz) and at EMR. Profiles of $\alpha_{E,L}$ vs f are shown in Fig. 4 for samples with a series of PZT concentration w . The features in Fig. 4 are similar to the data in Figs. 1 and 3 for layered samples. The PZT concentration dependence of low frequency and resonance α_E are also shown in Fig. 4. From the data one infers a dramatic strengthening of ME interaction at resonance; $\alpha_{E,L}$ increases by a factor of 600. The ME voltage coefficient at resonance

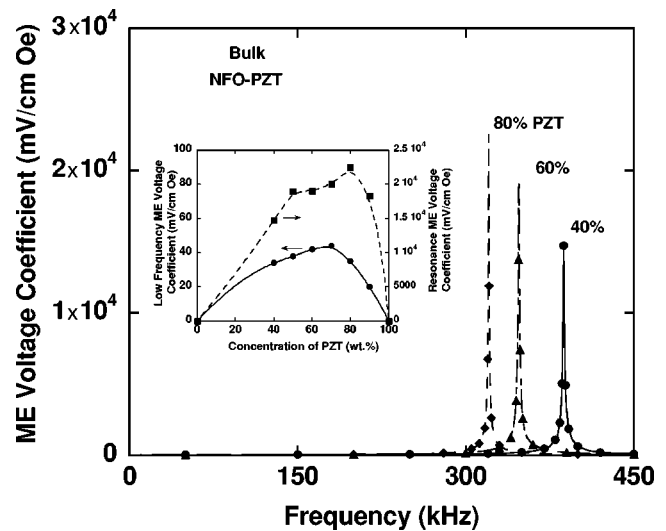


FIG. 4. $\alpha_{E,L}$ vs f data showing resonance in ME coupling at EMR for bulk nickel ferrite-PZT composites. The data are for samples with a series of PZT weight percent w . Inset shows off-resonance and resonance $\alpha_{E,L}$ as a function of w . The lines are guide to the eye.

is as high as 23000 mV/cm Oe. The overall increase in $\alpha_{E,L}$ at resonance is much higher in bulk samples than for layered systems. In conclusion, a theoretical model has been presented for magnetoelectric coupling at EMR in a ferromagnetic-ferroelectric layered system. The predicted giant ME interactions at resonance is in agreement with the data for ferrite-PZT samples.

This work was supported by grants from the Russian Ministry of Education (E02-3.4-278), the Universities of Russia Foundation (UNR 01.01.007), and the National Science Foundation (DMR-0302254).

¹L. D. Landau and E. M. Lifshitz, *Electrodynamics of Continuous Media* (Pergamon Press, Oxford, 1960), p. 119 (translation of Russian edition, 1958).
²D. N. Astrov, Zh. Eksp. Teor. Fiz. **40**, 1035 (1961) [Sov. Phys. JETP **13**, 729 (1961)].
³J. Van den Boomgaard, D. R. Terrell, and R. A. J. Born, J. Mater. Sci. **9**, 1705 (1974).
⁴J. Van den Boomgaard and R. A. J. Born, J. Mater. Sci. **13**, 1538 (1978), and references therein.
⁵G. Harshe, J. P. Dougherty, and R. E. Newnham, Int. J. Appl. Electromagn. Mater. **4**, 161 (1993).
⁶G. Harshe, J. P. Dougherty, and R. E. Newnham, Int. J. Appl. Electromagn. Mater. **4**, 145 (1993).

⁷G. Srinivasan, E. T. Rasmussen, and R. Hayes, Phys. Rev. B **67**, 014418 (2003).
⁸G. Srinivasan, E. T. Rasmussen, B. J. Levin, and R. Hayes, Phys. Rev. B **65**, 134402 (2002).
⁹J. Ryu, A. V. Carazo, K. Uchino, and H. Kim, Jpn. J. Appl. Phys. **40**, 4948 (2001).
¹⁰K. Mori and M. Wuttig, Appl. Phys. Lett. **81**, 100 (2002).
¹¹D. R. Tilley and J. F. Scott, Phys. Rev. B **25**, 3251 (1982).
¹²D. R. Tilley and J. F. Scott, Ferroelectrics **36**, 293 (1981).
¹³M. I. Bichurin, V. M. Petrov, Yu. V. Kiliba, and G. Srinivasan, Phys. Rev. B **66**, 134404 (2002).
¹⁴R. Bozorth, *Ferromagnetism* (IEEE Press, New York, 1993).